

Characterization of CuO/Polystyrene nanocomposite deposited by spin-coating technique

B. TROUDI, O. HALIMI*, M. SEBAIS, B. BOUDINE, A. DJEBLI

Laboratory of Crystallography, Department of Physics, University Freres Mentouri, Algeria

This work presents the results of an investigation on the structural and optical properties of CuO/polystyrene (CuO/PS) nanocomposite, prepared by a simple insertion of CuO nanoparticles into polystyrene (PS) matrix. CuO nanoparticles have been synthesized by a hydrothermal method, and thin films of CuO/PS nanocomposite have been deposited on glass substrate by spin-coating technique. X-ray diffraction and atomic force microscopy (AFM) have been used to study the structural and morphological properties of CuO/PS nanocomposite thin films. XRD have demonstrated the incorporation of monoclinic CuO nanoparticles in PS matrix and AFM micrographs have shown a homogeneous dispersion of CuO particles. The size of CuO particles was found to lie in the range 08.26 – 20.80 nm. FT-IR and Raman spectroscopy exhibit vibrational modes corresponding to the CuO monoclinic phase. The UV-visible absorption measurement indicates that the band gap energy of the CuO/PS nanocomposite thin films is 3.31 eV, and shows a significant blue-shift in the band gap energy of CuO, which is due to the quantum confinement effect performed by the CuO nanocrystals. Room temperature photoluminescence spectrum has shown that the insertion of CuO nanoparticles in PS matrix enhances the luminescence, in the visible range, of prepared CuO/PS nanocomposite.

(Received April 8, 2016; accepted February 10, 2017)

Keywords: Hydrothermal synthesis, CuO/PS nanocomposite, Photoluminescence.

1. Introduction

In the last years, many scientific works have been focused on the development of nanocomposite materials using different polymers and a variety of fillers. The interest accorded to the fabrication of nanocomposites is due to the possibility of obtaining materials with new properties for application in many areas of technology such as optoelectronics, electrochemistry, coating technology and catalysis [1]. The incorporation of inorganic nanoparticles into organic matrices can endow the resulting nanocomposites with excellent electrical, optical and mechanical properties [2,4]. The nanocomposite materials consisting of metal oxides and polymers exhibit the merits of blending the advantageous properties of metal oxides with the process ability and flexibility of polymers.

Among the important metal oxides, copper (II) oxide or cupric oxide (CuO) is an important p-type metal oxide semiconductor with a band gap of 1.2–2.5 eV [5,6]. It is the higher oxide of copper and it can be formed by heating copper in air: $2\text{Cu} + \text{O}_2 \rightarrow 2\text{CuO}$. It belongs to the monoclinic crystal system, with the space group C2/c and lattice parameters $a=4.6837 \text{ \AA}$, $b=3.4226 \text{ \AA}$, $c=5.1288 \text{ \AA}$, $\alpha=90^\circ$, $\beta=99.54^\circ$ and $\gamma=90^\circ$. The copper atom, in this structure, is coordinated by 4 oxygen atoms in an approximately square planar configuration [7]. CuO has acquired a certain interest thanks to its potential applications in electronic and optoelectronic devices due

to its particular optical and electrical properties in addition to its availability and non-toxicity.

The polystyrene (PS) with an optical gap of 4.2 eV [8] is a transparent polymer and it constitutes a suitable matrix for housing semiconductor nanoparticles with an optical activity in the visible range. The properties of filled polymer depend on several factors such as nature, concentration, size and morphology of the filler particles as well as their interaction with the polymer. Many methods have been described for the preparation of polymer nanocomposites, including layered materials and those containing nanoparticles [9]. The most important ones are: intercalation of the polymer or pre-polymer from solution, in-situ intercalative polymerization, melts intercalation, direct mixture of polymer and particles, template synthesis, in-situ polymerization and Sol-gel process. As it is known, the method of preparation influences the physical and chemical properties of materials.

So, in order to modify and improve their structural and optical properties, we present the investigation of thin films of CuO/PS nanocomposite which are synthesized by a direct addition of nanosized particles of CuO to PS, and that are deposited by spin-coating technique on glass substrates. Structural characterization of the samples was performed using XRD, AFM, FT-IR and micro-Raman spectroscopies, while the optical properties are evidenced using the optical absorption and photoluminescence.

2. Experimental

2.1. Preparation of samples

For the first step of samples preparation, we used the hydrothermal method for synthesizing nanoparticles of CuO. The chemical materials used were purchased from Aldrich and used as received without any further purification. In a typical synthesis process, 0.5 g of $\text{CuSO}_4 \cdot 5\text{H}_2\text{O}$ and 0.5 g of NaOH were dissolved into 40 mL of distilled water. Then, the mixture was magnetically stirred for 30 min. Thereafter, this solution was transferred into Teflon lined sealed stainless steel autoclave and maintained in an oven at a constant temperature of 200°C for 1 hour under autogenous pressure. The autoclave was allowed to cool naturally to room temperature. After the reaction was completed, the resulting black powder was washed with ethanol and distilled water, filtered and then dried in a laboratory oven at 80°C . During the second step we produce a colloidal solution of CuO/PS nanocomposite. The polystyrene ($\text{CH}_2=\text{CH}-\text{C}_6\text{H}_5$) is soluble in many organic solvents such as toluene, tetrahydrofuran (THF), acetone, benzene and, particularly, chloroform. In our work we dissolved the polystyrene in chloroform to get a colloidal solution (0.1 g/mL). This solution is heated to 50°C and stirred for 1 hour to improve the homogenization. On the other hand, another solution is prepared by introducing CuO nanoparticles (50 mg) in the chloroform solvent (10 mL). The obtained solution is stirred for 30 minutes to ensure a homogeneous dispersion and to prevent the agglomeration of CuO nanoparticles. In order to obtain the CuO/PS composite, we mix both solutions then the mixture is stirred for 30 mn. Mass proportions of the polystyrene and CuO nanoparticles in the solvent were chosen in a way to have a non-agglomerated, homogeneous and stable solution. In the third step, glass slides used as substrate were washed with ethanol and thoroughly rinsed with distilled water before the deposition of few droplets of CuO NCs doped PS solution.

Thin films were deposited by spin-coating technique performed under various conditions depending on the viscosity of the mixture. The rotational speed ranged from 300 to 2000 rpm in order to control the thickness. The deposition principle is based on homogeneous spreading using appropriate conditions. All experiments were performed at ambient pressure and room temperature.

2.2. Characterization techniques

The structural characterization of the deposited thin films of CuO/PS nanocomposite was performed on an X'pert PRO PANalytical X-ray diffractometer using $\text{CuK}\alpha$ radiation ($\lambda=1.54059\text{ \AA}$). The chemical analysis by Fourier transform infrared spectroscopy was carried out using a JASCO FT-IR 6300 spectrophotometer.

Raman spectra were recorded in a backscattering configuration with a RENISHAW 1000 micro-Raman spectrometer using an excitation wavelength of 633 nm (He-Ne laser) and an output of 10 mW. The surface morphology was studied by atomic force microscopy (AFM) using A100-AFM with SPM control system program version 6.4.3.

The optical properties were investigated by the UV-Visible absorption using a Shimadzu UV-3100PC Spectrophotometer and photoluminescence spectra were obtained by exciting the samples at room temperature with a radiation of 355 nm of third harmonic of Q-switched Nd:YAG laser. The luminescence was collected by an ANDOR SHAMROCK SR303i monochromator equipped with a grating blazed at 500 nm with 300 lines/mm, and analyzed with an iSTAR CCD.

3. Results and discussions

3.1. X-Ray diffraction analysis

X-ray diffraction patterns of undoped PS and CuO/PS nanocomposite thin films are shown in Fig. 1. Pure PS (spectrum (a)) exhibits no diffraction peaks; this means that it has an amorphous structure. However, for the CuO/PS (spectrum (b)) composite several diffraction peaks can be observed at $2\theta = 32.56, 35.60, 38.89, 48.86, 58.53, 61.80, 66.26, 68.20$ and 75.25 which may be assigned to the diffraction lines corresponding to the (110), (002), (200), ($\bar{2}$ 02), (202), ($\bar{1}$ 13), ($\bar{3}$ 11), (220) and ($\bar{2}$ 22) planes of monoclinic structure of CuO with lattice parameters : $a = 4.685\text{ \AA}$, $b = 3.423\text{ \AA}$, $c = 5.132\text{ \AA}$, $\beta = 99.52^\circ$ and space group C2/c in agreement with data reported in JCPDS card 41-0254 of CuO monoclinic. These peaks confirm the incorporation of CuO crystallites in PS matrix with a random orientation. The intensity of the main peaks reflects the good crystallization of the CuO particles.

All peaks belong to the monoclinic structure of CuO (no others peaks detected), which means that there was no chemical reaction and no new phase formation. Also, peaks have relatively wide profiles indicating that the crystallites have a small (nanometric) size. The sizes of CuO crystallites are estimated using the formula of Debye-Scherrer:

$$D = \frac{0.89 \lambda}{\beta \cos \theta}$$

Where λ is the wavelength of X-Ray (0.154059 nm), β is the FWHM (full width at half maximum), θ is the diffraction angle and D is the size of particles. The average crystallite size is found in the range 8.26-20.80 nm (Table 1).

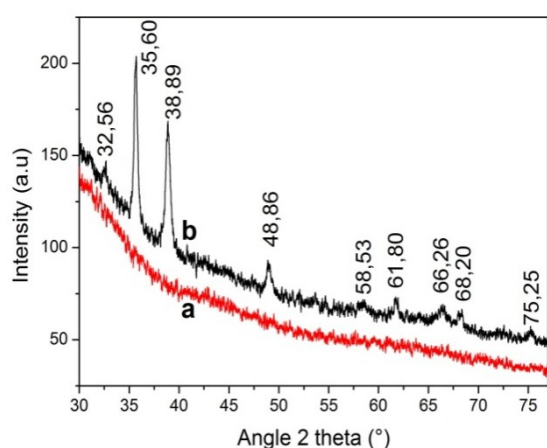


Fig. 1. X-Ray spectra of (a)-pure PS and (b)-CuO/PS nanocomposite

Table 1. Nanometric sizes of CuO nanocrystals embedded in PS matrix

2θ (°)		(hkl)	FWHM (°)	Size (nm)
Observed	Reported			
32.56	32.50	(110)	0.58	14.11
35.60	35.43	(002)	0.40	20.62
38.89	38.94	(200)	0.56	14.87
48.86	48.74	($\bar{2}$ 02)	0.64	13.48
58.53	58.31	(202)	1.07	08.26
61.80	61.54	($\bar{1}$ 13)	0.44	20.80
66.26	66.27	($\bar{3}$ 11)	1.04	09.02
68.20	68.14	(220)	0.78	12.16
75.25	75.26	($\bar{2}$ 22)	0.59	16.84

3.2. AFM Analysis

For more information on the structural properties of CuO/PS nanocomposite thin films, we have analyzed the topography of their surface and the distribution of CuO nanoparticles. The AFM technique is applied to investigate the surface profiles of the films. Figures 2a and 2b show respectively, three-dimensional (3D) and two-dimensional (2D) topographical images of CuO/PS nanocomposite. CuO particle aggregates are clearly visible on the surface of the films. These aggregates of different sizes are uniformly spread.

The height of particles (Fig. 2a) reflects the particles size and highlights that the aggregates are formed by nanosized CuO particles. The line profile (Figure 2c) obtained by Gwyddion-2.39.win32.exe software [10] reveals that the approximate size of CuO particles is around 14 nm. This result is coinciding with that of X-ray investigation.

AFM analysis reveals, from the 3D micrographs, the agglomeration and homogeneous distribution of CuO particles. The surface roughness of CuO/PS

nanocomposite thin films was estimated to 2.6 nm. The AFM images show well that the surface morphology and surface roughness of the films are strongly dependent on the crystallite size variations.

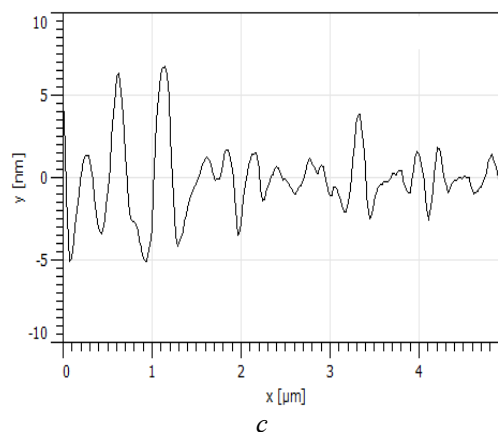
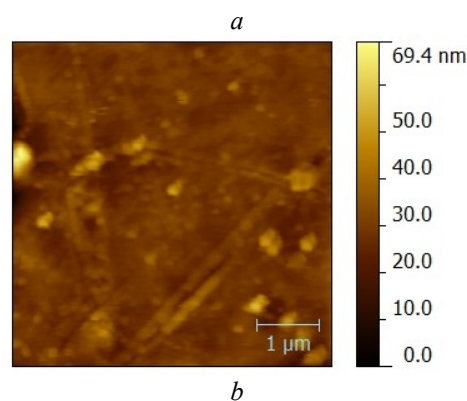
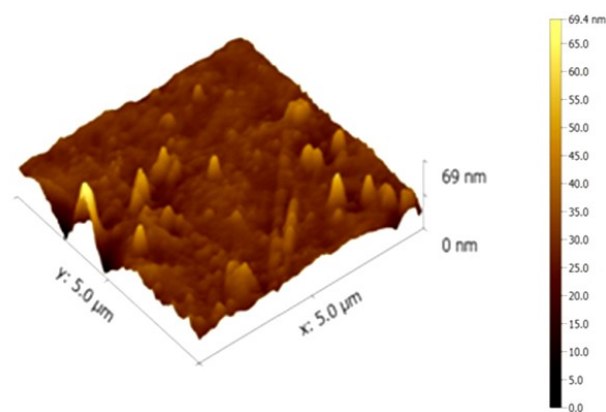


Fig. 2. AFM image (5 μm x 5 μm) of as prepared CuO/PS nanocomposite thin film: (a)-3D, (b)-2D, and (c)-line profile

3.3. Raman analysis

As it is known, the monoclinic structure of CuO belongs to the C_{2h}^6 space group with two molecules per primitive cell which allowed 12 vibrational modes: 4Au + 5Bu + Ag + 2Bg. Among these modes only three are Raman active modes: Ag + 2Bg [11]. On the Raman spectrum of the CuO/PS nanocomposite (Fig. 3), we can see three bands at positions 292, 342 and 624 cm^{-1} , which

are assigned to the standard Ag, Bg(1) and Bg(2) modes and the positions are in good agreement with that reported by Thi Ha Tran and Viet Tuyen Nguyen [12]. In Table 2, our results are compared with data previously reported [13, 14].

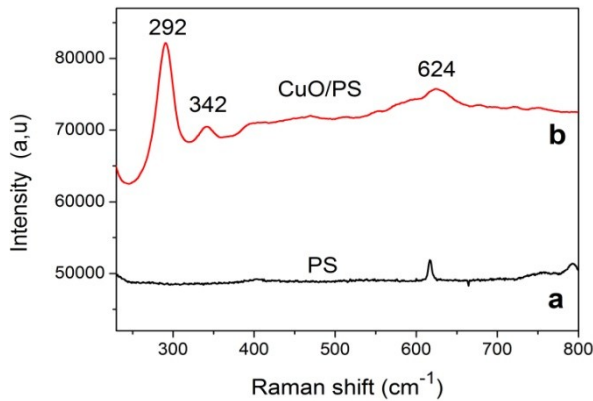


Fig. 3. Compared Raman spectra of (a)-PS pure and (b)-CuO/PS nanocomposite

Table 2. Compared frequencies of vibration modes of CuO

Vibrational mods assignement	Wave number (cm ⁻¹) [13]	Wave number (cm ⁻¹) [14]	Wave number (cm ⁻¹) [12]	Wave number (cm ⁻¹) [Work]
Ag	298	295.2	295	292
Bg(1)	340	342.7	343	342
Bg(2)	626	633.5	629	624

3.4. FT-IR Analysis

FT-IR spectroscopy allows a chemical analysis of materials by measuring the vibrational frequency of the bonds in the molecular groups. The FT-IR spectrum of CuO/PS thin film nanocomposite is shown in Fig. 4. The peaks observed at around 605 and 528 cm⁻¹ are due to stretching of bond Cu-O along of the direction $\bar{2}02$ as reported by Dar M.A. et al [15]. Those observed at 487 and 435 cm⁻¹ are assigned to stretching of bond Cu-O along of the direction 202 [16, 20]. The peak at 582 cm⁻¹ is attributed to stretching of bond Cu-O along of the direction $\bar{1}01$ [21]. M Abaker et al have also observed a vibrational mod at about 502 cm⁻¹ for bond Cu-O [22].

These vibrational modes observed for the Cu-O bond in the prepared CuO/PS nanocomposite have also been reported in other works on the CuO compound, but with a weak shift caused by the size and morphology of particles which depend on the synthesis method and the treatments post-synthesis [23, 29].

The results of the analysis by Raman and infrared spectroscopy reaffirm the incorporation of CuO nanoparticles with monoclinic structure in the host matrix of polystyrene.

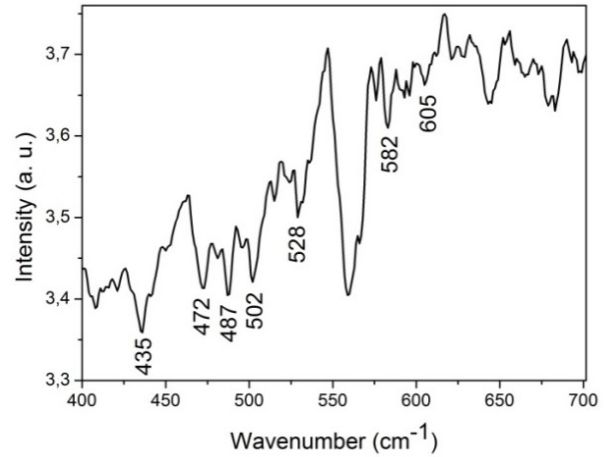


Fig. 4. FT-IR spectrum of CuO/PS nanocomposite

3.5. Optical absorption analysis

Optical absorption in the UV-Visible region is used to study changes in the energy of the optical gap for thin films of pure PS and CuO/PS nanocomposite. The shifting of the optical gap depends on some experimental conditions such as temperature, concentration of precursors, nature of solvents and defects of the material. Any variation in such parameters leads to a shift of the absorption edge toward higher or lower energies. In our work, optical absorption measurements were performed on samples of pure PS and of CuO/PS nanocomposite. Measurements were undertaken at ambient temperature in the UV-Visible range for the pure PS and in the range from 350 to 750 nm for the CuO/PS nanocomposite which corresponds to the transparent region of polystyrene matrix. The UV-Visible absorption spectra of thin films of pure PS and CuO/PS nanocomposite are respectively shown in Fig. 5 and Fig. 6.

For the pure PS films, there is no appreciable absorption in the visible range (Fig. 5a) but we note, in the UV range, two absorption peaks at 283 and 292 nm which are characteristic of Polystyrene [30]. We also notice a steep absorption edge at around 274 nm. The value of the band gap energy, determined using the second derivative method [31], is 4.24 eV (Fig. 5b). It is in agreement with band gap of PS (4.20 eV) reported by Alwan et al [8].

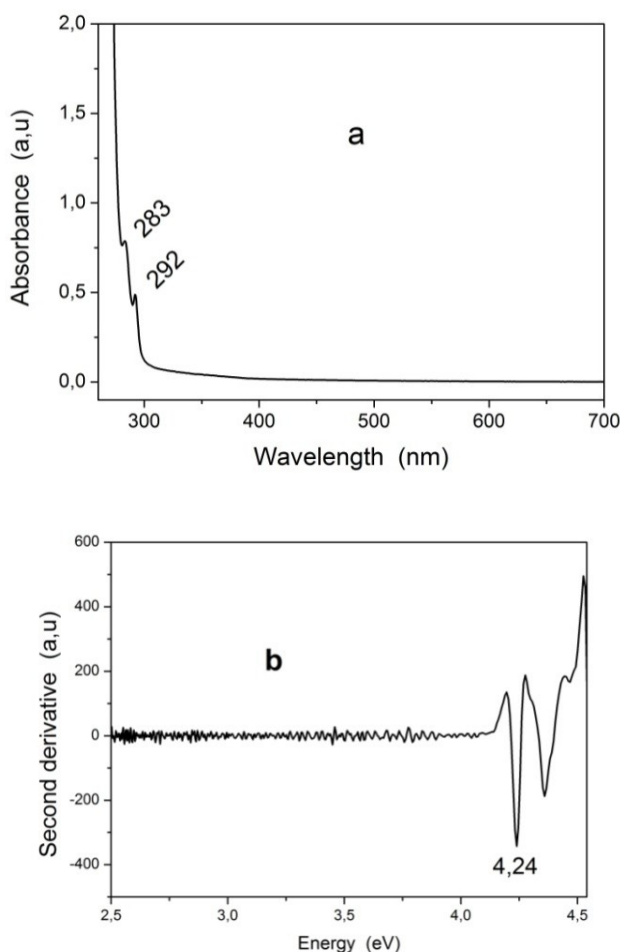


Fig. 5. UV-Visible absorption spectrum of pure PS film (a)-Absorbance versus wavelength, (b)-Optical Gap of PS

Furthermore, we note the presence of absorption bands at 372, 405, 504 and 661 nm for the CuO/PS nanocomposite (Fig. 6a). The first one at 372 nm is due to the direct band to band transitions [32, 33]. The band at 405 nm is from near band edge transitions and it is in agreement with absorption of CuO nanoparticles embedded in polyaniline as reported by Jundale D. M. et al [34], whilst the band situated at 505 nm is associated with oxygen vacancies in the CuO nanocrystals [35]. The band at 661 nm is ascribed to the presence of interstitial defects of CuO [36]. These positions of absorption bands are shifted from that reported for CuO particles in earlier works [37, 39] and this indicates that the insertion of CuO nanoparticles in PS matrix has an effect on the optical band gap of CuO/PS nanocomposite.

The band gap energy for the CuO/PS nanocomposite has been estimated using the second derivative of absorbance [31]. The value found is 3.31 eV (Figure 6c), it is in agreement with the value of 3.35 eV observed by Xinhong Zhao et al [40]. The found gap is lower than that of PS but higher than that of bulk CuO. This result indicates that the doping of a PS polymer matrix by CuO

nanoparticles induces a red shift of the band gap energy compared with that of polystyrene and a blue shift compared with that of bulk CuO. This blue-shift is caused by the well-known quantum confinement effect seen that the Bohr radius 28.27 nm [29] of CuO semiconductor is larger than the size of CuO nanoparticles (Table 1). In addition to the quantum confinement effect induced by the nanometric size of CuO particles, the changes in the band gap energy are also caused by the interaction at the interface of host PS and CuO nanoparticles [41, 43].

Finally, the band gap energy of CuO/PS nanocomposite depends on parameters like the gap of PS, gap of CuO, size of CuO nanoparticles and interaction characteristics between CuO nanoparticles and PS host matrix.

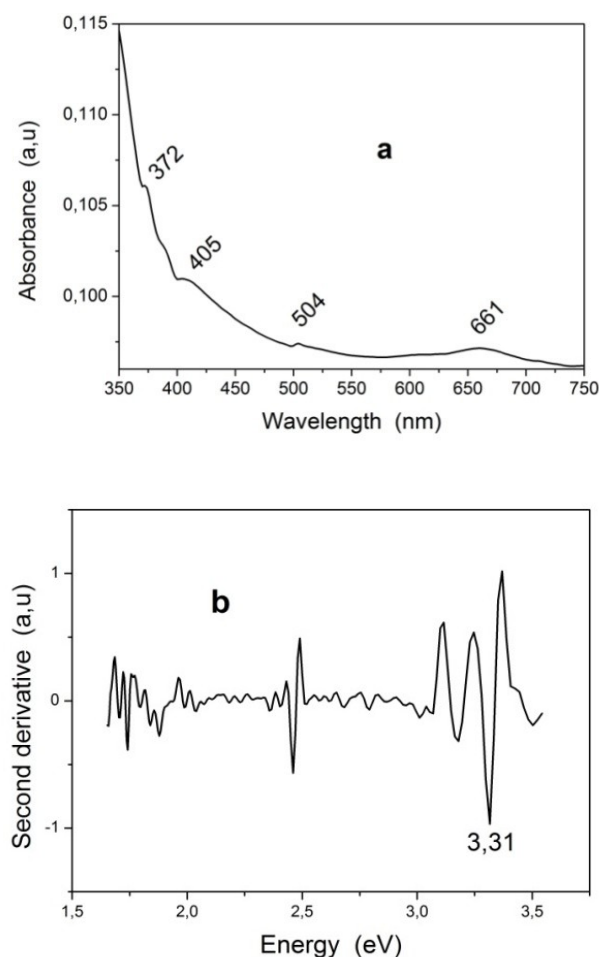


Fig. 6. UV-Visible absorption spectrum of CuO/PS nanocomposite: (a)- Absorbance versus wavelength (b)-Optical gap of CuO/PS nanocomposite

3.6. Photoluminescence analysis

The photoluminescence spectrum, at room temperature of prepared CuO/PS nanocomposite, is shown in Fig. 7 after excitation with a wavelength of 355 nm. It covers the entire visible range with three distinct bands

centred at 465, 525 and 680 nm. These emission bands are consistent with absorption measurements [25]. Various factors are often involved in setting up the photoluminescence spectrum of a given material. In the visible range, PL emission is mainly attributed to the presence of defects like vacancies or impurities of materials.

For the copper oxide CuO, vacancies may be copper or oxygen vacancies while the impurities may be interstitial copper or anti-oxygen sites O_{Cu} [35]. These defects induce the formation of new energy levels in the band gap and, as a result, emissions will arise from these trapped levels during excitation of the sample. Emission occurs due to radiative recombination of a photo-excited hole with an electron and the emission bands are commonly referred to as deep level or trap site emission due to oxygen vacancies [44].

As it is known, CuO is intrinsically a p-type semiconductor due to the existence of Cu vacancies, so the emission by CuO is essentially due to this type of defects. However, recent theoretical calculations indicate that although Cu vacancies are the most stable defects in CuO, they do not make any changes in the electronic structures of CuO. Otherwise, oxygen vacancies or O_{Cu} antisite defects are likely responsible of CuO emissions seeing that their formation energy is not much different from the formation energy of Cu vacancies [45]. The study of the emission bands of prepared CuO/PS nanocomposite, and the comparison of our experimental results with that reported in some earlier works on luminescence of CuO nanoparticles [46, 47], allow to assign the emission band in the blue region (465 nm) to the near band edge emission (NBE) of CuO [25]. This near-band-edge emission is attributed to emission originated from the recombination of electrons and holes of free excitons in CuO that is quantum-mechanically very sensitive to particles size.

The blue shift behavior of the near band edge transition in comparison with that of the bulk CuO in combination with the findings from UV-visible analysis is normally attributed to the enhancement of the quantum confinement effect resulting from the decrease in the dimensional structure and the size of the nanoparticles [12]. The near band edge emission (NBE) of CuO particles arises at different wavelengths as reported by Ibrahim Y. Erdogan et al in the blue region [25] at 467 nm, by Mukherjee et al at 395 nm in the violet region [46] and by Alireza Aslani at 300 nm [48]. This means that the factors at the origin of the blue luminescence of CuO nanoparticles are not yet well established. The green emission band at 525 nm results from the singly ionized oxygen vacancy of CuO material following the recombination of a photo generated hole with a singly ionized electron in the valence band [32].

This intense (green) emission indicates a large concentration of surface defects associated with oxygen vacancies that is in agreement with the large surface/volume ratio of CuO nanoparticles.

This deduction is in accordance with the nanoscale size of CuO particles found by XRD analysis (Table 1). The red emission at 680 nm has been supposed to relate to the interstitial metal ion in the oxide [49]. It is generally accepted that the green and red emissions are associated with oxygen vacancies and interstitial metal ions in the oxide CuO [50, 53].

The intensity of the emission bands depends on factors such as polymer coil size, nature of polymer-solvent, polymer-dopant interactions and the degree of chain overlapping [54].

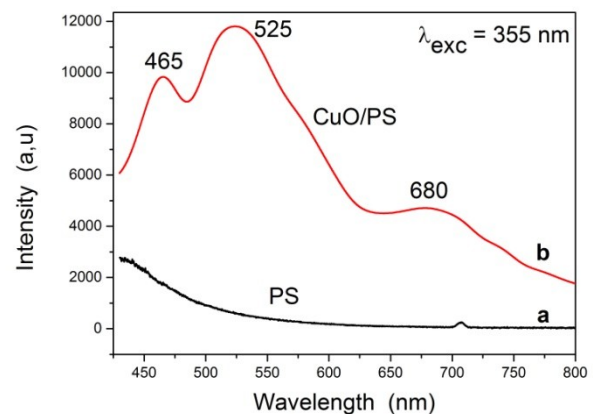


Fig. 7. Compared PL spectra of (a)-PS and (b)-CuO/PS nanocomposite

4. Conclusion

In the present work, we have reported the synthesis with structural and optical study of hybrid nanocomposite CuO/PS. CuO nanoparticles synthesized by a hydrothermal method were dispersed in polystyrene to fabricate thin films of CuO/PS nanocomposite by spin-coating method. Structural analysis by XRD revealed the incorporation into the PS host matrix of monoclinic CuO nanocrystals, with an average crystallite size of about 14.76 nm. The analysis by Raman and FT-IR spectroscopies showed the presence of Cu–O vibration modes and so confirm the result of XRD analysis on the formation of CuO/PS nanocomposite. Furthermore, the AFM images show a homogeneous distribution of CuO nanoparticles. The optical absorption in the UV-Visible range displays characteristic absorption bands of CuO nanoparticles and exhibits a blue shift of the absorption edge compared with that of bulk CuO, which is a consequence of the quantum confinement effect of charges in CuO induced by the nanometric size of CuO particles. The PL spectrum shows three emission bands: blue, green and red which occur from energy levels corresponding to structural trapped defects. The insertion of CuO nanoparticles in the PS matrix allows the obtention of a composite with specific optical properties which can be used in the manufacture of new optical devices.

References

- [1] P. H. C. Camargo, K. G. Satyanarayana, F. Wypych, *Materials Research* **12**(1), 1 (2009).
- [2] R. Shenhar, T. B. Norsten, V. M. Rotello, *Advanced Materials* **17**(6), 657 (2005).
- [3] D. R. Paul, L. M. Robeson, *Polymer* **49**(15), 3187 (2008).
- [4] A. Lagashetty, A. Venkataraman, *Resonance* **10**(7), 49 (2005).
- [5] N. Wang, H. He, L. Han, *Applied Surface Science*, **256**, 7335 (2010).
- [6] A. H. Jayatissa, K. Guo, A.C. Jayasuriya, *Appl. Surf. Sci.*, **255**, 9474 (2009).
- [7] J. B. Forsyth, S. J. Hull, *Phys. Condens. Matter* **3**, 5257 (1991).
- [8] T. J. Alwan, *Malaysian Polymer Journal* **5**(2), 204 (2010).
- [9] S. Kango, S. Kalia, A. Celli, J. Njuguna, Y. Habibi, R. Kumar, *Progress in Polymer Science* **38**(8), 1232 (2013).
- [10] Gwyddion development. Scanning probe microscopy (2009). <http://gwyddion.net/> (accessed 08-03-2016).
- [11] C. Prakash, G. Anurag, K. Ashavani, K. G. Umesh, *Materials Science in Semiconductor Processing* **38**, 72 (2015).
- [12] T. H. Tran, V. T. Nguyen, A Brief Review; *International Scholarly Research Notices*, 2014, Article ID 856592, 14 pages. (2014).
- [13] K. M. Chahrour, N. M. Ahmed, M. R. Hashim, G. Nezar Elfadill, M. Bououdina, *Sensors and Actuators A* **239**, 209 (2016).
- [14] T. Yu, X. Zhao, Z. X. Shen, Y. H. Wu, W. H. Su, *Journal of Crystal Growth* **268**, 590 (2004).
- [15] M. A. Dar, Y. S. Kim, W. B. Kim, J. M. Sohn, H. S. Shin, *Applied Surface Science* **254**, 7477 (2008).
- [16] M. A. Dar, S. H. Nam, Y. S. Kim, W. B. Kim, *Journal of Solid State Electrochemical* **14**, 1719 (2010).
- [17] Y. Li, Q. Zhang, J. Li, *Talanta* **83**, 162 (2010).
- [18] M. Guedes, J. M. F. Ferreira, A. C. Ferro, *J. Colloid Interf. Sci.* **330**, 119 (2009).
- [19] L. Chen, L. Li, G. Li, *Journal of Alloys and Compounds* **464**(1-2), 532 (2008).
- [20] D. M. Fernandes, R. Silva, A. Hechenleitner, E. Radovanovic, M. A. C. Melo, E. A. G. Pineda, *Materials Chemistry and Physics* **115**(1), 110 (2009).
- [21] R. Abdul, I. Amri, J. Desi, M. Stella, S. Hanggara, *Indonesian Journal of Chemistry* **9**(3), 355 (2009).
- [22] M. Abaker, A. Umar, S. Baskoutas, S. H. Kim, S. W. Hwang, *J. Phys. D: Appl. Phys.* **44**, 155405 (2011).
- [23] M. Fterich, F. Ben Nasr, R. Lefi, M. Toumi, S. Guerhazi, *Materials Science in Semiconductor Processing* **43**, 114 (2016).
- [24] A. S. Padampalle, A. D. Suryawanshi, V. M. Navarkhele, D. S. Birajdarn, *International Journal of Recent Technology and Engineering* **2**(4), 19 (2013).
- [25] I. Y. Erdogan, O. Gullu, *Journal of Alloys and Compounds* **492**, 378 (2010).
- [26] N. Bouazizi, R. Bargougui, A. Oueslati, R. Benslama, *Adv. Mater. Lett.* **6**(2), 158 (2015).
- [27] Y. Xu, D. Chen, X. Jiao, *J. Phys. Chem. B* **109**(28), 13561 (2005).
- [28] K. J. Arun, A. K. Batra, A. Krishna, K. Bhat, M. D. Aggarwal, P. J. J. Francis, *American Journal of Materials Science* **5**(3A), 36 (2015).
- [29] M. Abdul Momin, R. Pervin, M. Jalal Uddin, G. M. A. Khan, M. Islam, *J. Bangladesh Electron* **10**(1-2), 57 (2010).
- [30] T. Li, C. Zhou, M. Jiang, *Polymer Bulletin* **25**, 211 (1991).
- [31] A. Othmani, J. C. Plenet, E. Berstein, C. Bovier, J. Dumas, P. Riblet, P. Gilliot, R. Levy, J. B. Grun, *Journal of Crystal Growth* **144**, 141 (1994).
- [32] S. L. Amrut, J. S. Satish, B. P. Ramchandara, S. N. Raghmani, *Advances in Applied Science Research* **1**(2), 36 (2010).
- [33] R. M. Mohamed, F. A. Hazz, A. Shawky, *Ceramics International* **40**, 2127 (2014).
- [34] D. M. Jundale, S. T. Naval, G. D. Khuspe, D. S. Dalavi, P. S. Patil, V. B. Patil, *Journal of Materials Science: Materials in Electronics* **24**(9), 3526 (2013).
- [35] R. Divya, M. Meena, C. K. Mahadevan, C. M. Padma, *Int. Journal of Engineering Research and Applications* **4**(5), 01 (2014).
- [36] W. Wang, L. Wang, H. Shi, Y. Liang, *Cryst. Eng. Comm.* **14**, 5914 (2012).
- [37] S. Addala, L. Bouhdjar, A. Chala, A. Bouhdjar, O. Halimi, B. Boudine, M. Sebais, *Chin. Phys. B* **22**(9), 098 (2013).
- [38] D. Jundale, S. Pawar, M. Chougule, P. Godse, S. Patil, B. Raut, S. Sen, V. Patil, *Journal of Sensor Technology* **1**, 36 (2011).
- [39] R. Shabu, A. M. E. Raj, C. Sanjeeviraja, C. Ravidhas, *Materials Research Bulletin* **68**, 1 (2015).
- [40] X. Zhao, P. Wang, Z. Yan, N. Ren, *Optical Materials* **42**, 544 (2015).
- [41] D. N. Huyen, N. T. Tung, N. D. Thien, L. H. Thanh, *Sensors* **11**, 1924 (2011).
- [42] L. Cindrella S. Prabhu, *Applied Surface Science* **378**, 1 (2016).
- [43] J. K. Rao, A. Raizada, D. Ganguly, M. M. Mankad, S. V. Satyanarayana, G. M. Madhu, *J. Mater. Sci.* **50**, 7064 (2015).
- [44] R. Divya, M. Meena, C. K. Mahadevan, C. M. Padma, *International Journal of Engineering Research & Technology* **3**(7), 1 (2014).
- [45] D. Wu, Q. Zhang, M. Tao, *Physical Review B-Condensed Matter and Materials Physics* **73**(23), 235206. (2006).
- [46] N. Mukherjee, B. Show, S. K. Maji, U. Madhu, S. K. Bhar, B. C. Mitra, G. G. Khan, A. Mondal, *Mater. Lett.* **65**, 3248 (2011).
- [47] K. Mageshwari, R. Sathyamoorthy, *J. Mater. Sci. Technol.* **29**(10), 909 (2013).
- [48] A. Aslani, *Physica B* **406**, 150 (2011).

- [49] S. Dagher, Y. Haik, A. I. Ayesh, N. Tit, *Journal of Luminescence* **151**, 149 (2014).
- [50] L. Spanhel, M. A. Anderson, *J. Am. Chem. Soc.* **113**, 2826 (1991).
- [51] D. M. Bagnall, Y. F. Chen, M. Y. Shen, Z. Zhu, T. Goto, T. Yao, *J. Cryst. Growth* **184/185**, 605 (1998).
- [52] S. A. Studenikin, N. Golego, M. Cocivera, *J. Appl. Phys.* **84**, 2287 (1998).
- [53] K. Vanheusden, W. L. Warren, C. H. Seager, D. R. Tallant, J. A. Voigt, B. E. Gnade, *J. Appl. Phys.* **79**, 7983 (1996).
- [54] S. K. Singh, A. K. Verma, R. Lakhan, R. K. Shukla, *International Journal of Management, Information Technology and Engineering* **2(7)**, 85 (2014).

*Correspondant author: h.ouahiba@yahoo.fr